Phase-Variation Microwave Sensor for Permittivity Measurements Based on a High -Impedance Half-Wavelength Transmission Line

Lijuan Su, *Member*, *IEEE*, Jonathan Muñoz-Enano, *Student Member*, *IEEE*, Paris Vélez, *Member*, *IEEE*, Pau Casacuberta, Marta Gil, and Ferran Martín, *Fellow*, *IEEE*

***Abstract*—A phase-variation microwave sensor operating in transmission and implemented by means of a high-impedance half-wavelength sensing line is reported in this paper. The sensor is useful for dielectric constant measurements and dielectric characterization of materials. By forcing the electrical length of the sensing line to be a half-wavelength when it is loaded with the so-called reference (REF) material, perfect matching is obtained regardless of the characteristic impedance of the line. This fact can be used to enhance the sensitivity for small perturbations, by merely increasing the characteristic impedance of the sensing line. An exhaustive analysis that supports such conclusion is reported in the paper. Then, two prototype sensors are designed and fabricated for validation purposes. As compared to the ordinary phase-variation permittivity sensor implemented by means of a matched (50-Ω) line with identical length, the sensitivity for small perturbations in the proposed sensor is 2.1 times larger. Further advantages of these sensors are low-cost, small size, implementation in planar technology, and very simple design and fabrication, derived from the fact that the sensing region is a half-wavelength transmission line.**

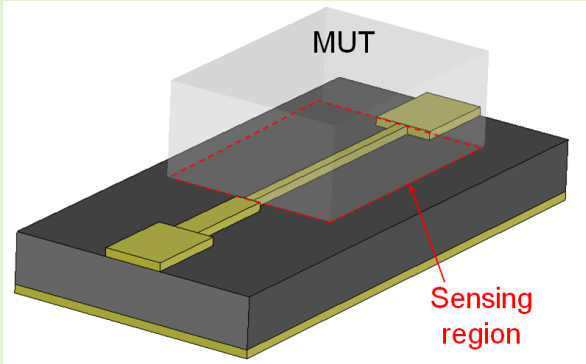

***Index Terms*—Dielectric characterization, microstrip technology, microwave sensors, permittivity sensors, phase-variation sensors.**

I. Introduction

THE RESEARCH activity devoted to performance improvement and size/cost reduction in planar sensors based on microwave technologies has experienced a significant growth in recent years. Microwave sensors are especially suited for material characterization since microwaves are very sensitive to the properties of the materials to which they interact. Coaxial probes [1]-[4] or resonant cavities [5]-[10] are well-known examples of microwave devices useful for material sensing and dielectric characterization. However, many applications demand sensor implementation in planar technology. The reasons are multiple, including low cost, low profile, possibility of sensor implementation in flexible substrates (e.g., for conformal sensors [11],[12]), compatibility with fully planar fabrication technologies (including also additive, i.e., printing, processes), and easy combination with other sensing technologies (e.g., microfluidics [13]-[16], wearables [17], lab-on-a-chip [18], organ-on-a-chip [19], organic and paper based sensors [20], etc.).

Many planar microwave sensors devoted to dielectric characterization and permittivity measurements are based on resonator-loaded transmission lines and exploit frequency variation [21]-[36]. In such devices, the sensing element is a planar resonator, sensitive to the complex permittivity of the material, or liquid, under test (MUT), which should be placed in contact with the sensing resonator, or in close proximity to it. The main limitative aspect of frequency-variation sensors is the need to generate a sweeping frequency signal able to cover the entire output dynamic range (the output variable in such sensors is the resonance frequency and, eventually, the peak or notch magnitude). For the generation of such frequency-varying signals, voltage controlled oscillators (VCOs) are typically used, representing a high cost solution for wideband output dynamic ranges. Wideband VCOs are also needed in the

This work was supported by MICINN-Spain (projects TEC2016-75650-R and PID2019-103904RB-I00), by Generalitat de Catalunya (project 2017SGR-1159), by Institució Catalana de Recerca i Estudis Avançats (who awarded Ferran Martín), and by ERDF. J. Muñoz-Enano acknowledges Secreteraria d'Universitats i Recerca (Gen. Cat.) and European Social Fund for the FI grant. Paris Vélez and Lijuan Su acknowledge the Juan de la Cierva Program for supporting them through Projects IJCI-2017-31339 and IJC2019-040786-I, respectively.

L. Su, J. Muñoz-Enano, P. Vélez, P. Casacuberta and F. Martín are with GEMMA/CIMITEC, Departament d'Enginyeria Electrònica, Universitat Autònoma de Barcelona, 08193 Bellaterra, Spain. E-mail: Ferran.Martin@uab.es.

M. Gil is with Departamento Ingeniería Audiovisual y Comunicaciones, Universidad Politécnica de Madrid, 28031 Madrid, Spain.

so-called frequency-splitting sensors [37]-[44]. In these sensors (similar to differential-mode sensors [45]-[57]), a line is loaded with a pair of identical resonators, sensitive to the difference in the material characteristics between the MUT and the reference (REF) sample.

It is clear that a significant reduction in the associated sensor electronics is achievable if a single-tone harmonic (interrogation) signal suffices for sensing. Both the phase and the magnitude of either the transmission or the reflection coefficient of a resonator-loaded, or ordinary, line at a fixed (predefined) frequency are expected to vary with the complex permittivity of the MUT. Therefore, such variables can be used for sensing in the so-called single-frequency sensors. Coupling-modulation sensors [58]-[68] and phase-variation sensors [69]-[78] belong to the category of single-frequency sensors. The magnitude and the phase of the transmission or reflection coefficient are the output variables in coupling-modulation and phase-variation sensors, respectively.

Coupling-modulation sensors are robust against cross-sensitivities caused by variations in environmental factors (such as temperature and humidity) [79]. However, such sensors exhibit limited tolerance against the effects of electromagnetic interference and noise, as compared to phase-variation sensors. Thus, in applications where the ambient conditions are not expected to vary significantly (or are not expected to significantly cause appreciable changes in the properties of the MUT), phase-variation microwave sensors constitute a very good option.

Single-ended [69] and differential-mode [70] phase-variation microwave sensors operating in transmission and implemented by means of matched ordinary or meandered lines have been recently reported. In such sensors, the sensitivity is proportional to the length of the sensing lines. Thus, for size reduction, strategies based on controlling the dispersion (dispersion engineering) in artificial lines, including composite right/left handed lines [45], electro-inductive-wave transmission lines [53], and slow-wave transmission lines [77],[78], have been reported. The resulting sensors exhibit competitive size and sensitivity. However, the design of these sensors is not exempt of certain complexity, as far as artificial lines [80] are involved. Recently, reflective-mode phase-variation microwave sensors based on either a half- or a quarter-wavelength open-ended sensing line cascaded to a set of 90º line sections with alternating high/low characteristic impedance, have been reported [73]. Excellent sensitivities with small sensing regions are achieved in these sensors, thanks to the multiplicative effect on the sensitivity caused by the impedance contrast of the high/low impedance 90º line sections.

In this paper, the objective is to optimize the sensitivity in transmission-mode sensors based on ordinary lines, by considering as design variables the characteristic impedance and the electrical length of the line section corresponding to the sensing region, not necessarily coincident with the whole sensor line. The work is organized as follows. Section II presents the proposed phase-variation microwave sensor and the working principle. The sensitivity analysis, devoted to find the optimum conditions for sensitivity optimization is carried out in Section III. From the conclusions inferred from such analysis, two microstrip prototype sensors are designed and validated by simulation and experiment, and the results are presented in Section IV. Finally, the main conclusions of the work are highlighted in Section V.

II. THE PROPOSED PHASE-VARIATION SENSOR AND WORKING PRINCIPLE

The schematic of the proposed sensor is depicted in Fig. 1. It is a two-port device consisting of a pair of cascaded line sections. The sensitive part of the sensor is the line section with characteristic impedance and electrical length designated as Z_s and ϕ_s, respectively. The MUT should be placed on top of the sensing region only, delimited by the dashed rectangle in Fig.1. The line section with impedance Z and electrical length ϕ is cascaded to the sensing line in order to increase the degrees of freedom, with the aim of enhancing the sensitivity as much as possible without the need of elongating the length of the sensing line (the trivial approach [70]). It is obvious that the electrical length and characteristic impedance of the sensing line depend on the dielectric constant of the MUT placed on top of it. These parameters, in turn, contribute to the value of the phase of the transmission coefficient, the considered output variable of the proposed sensor, and an easily measurable quantity.

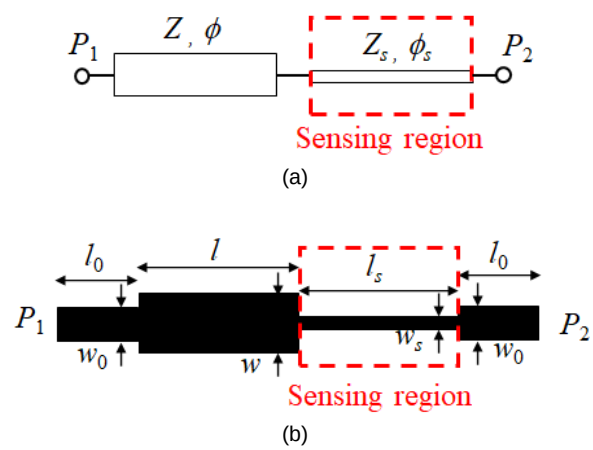

Fig. 1. Schematic (a) and typical topology in microstrip technology (b) of the proposed transmission-mode phase-variation dielectric constant sensor.

In uniform lines matched to the ports, the phase of the transmission coefficient coincides with the electrical length of the line. When designing a sensor based on a uniform line, the frequency of operation, f_0, must be set to a certain value, and a reference (REF) MUT should be decided. The electrical length of the line depends on that frequency, and also on the effective dielectric constant (determined by the transverse geometry of the line, by the dielectric constant of the substrate, and by the dielectric constant of the REF MUT). The characteristic impedance of the line, the relevant parameter for matching purposes, is also determined by the dielectric constant of the MUT. Therefore, in order to obtain line matching, thereby avoiding reflections, the line impedance should be forced to coincide with the reference impedance of the ports, Z_0, when the line is loaded with the REF MUT. These sensors are especially suited for the characterization of materials

experiencing small changes (equivalent to small perturbations) with regard to the REF MUT, since, in this case, quasi-matching conditions are preserved.

However, by considering a phase-variation sensor based on a cascade of several line sections, where at least one of such sections is the sensitive part, it is expected that the phase of the transmission coefficient, the output variable, exhibits a more complex dependence with the phase (electrical length) and characteristic impedance of the sensing line(s). Thus, it is potentially possible to obtain a stronger dependence of the output variable (the phase of the transmission coefficient) with the dielectric constant of the MUT sample, the input variable. This is the main aspect to study in the next section, devoted to the sensitivity analysis of the proposed sensor, which specifically consists of two line sections, one of them acting as sensitive part, as indicated before.

III. SENSITIVITY ANALYSIS

Let us first consider a sensor based on a single uniform sensing line with impedance Z_s and phase ϕ_s (i.e., let us exclude the presence of the cascaded line of Fig. 1). The phase of the transmission coefficient, ϕ_T, depends on both Z_s and ϕ_s, which, in turn, are influenced by the dielectric constant of the MUT, ε_{MUT}. Thus, the sensitivity can be expressed as

$$S = \frac{d\phi_T}{d\varepsilon_{MUT}} = \frac{d\phi_T}{d\phi_S}\cdot\frac{d\phi_S}{d\varepsilon_{MUT}} + \frac{d\phi_T}{dZ_S}\cdot\frac{dZ_S}{d\varepsilon_{MUT}} \tag{1}$$

In order to calculate (1), it is first necessary to obtain the transmission coefficient of the structure, S_{21}, which can be expressed in terms of the elements of the *ABCD* transmission matrix according to [80],[81]

$$S_{21} = \frac{2}{A + \frac{B}{Z_0} + CZ_0 + D} \tag{2}$$

with

$$\begin{pmatrix} A & B \\ C & D \end{pmatrix} = \begin{pmatrix} \cos\phi_s & jZ_S\sin\phi_S \\ jY_S\sin\phi_S & \cos\phi_s \end{pmatrix} \tag{3}$$

and $Y_s = 1/Z_s$. Introducing the elements of (3) in (2), the transmission coefficient is found to be

$$S_{21} = \frac{1}{\cos\phi_S + j\frac{1}{2}(\frac{Z_S}{Z_0} + \frac{Z_0}{Z_S})\sin\phi_S} \tag{4}$$

and the phase of S_{21} is

$$\phi_T \equiv \phi_{S_{21}} = -\arctan\left\{\frac{1}{2}(\frac{Z_S}{Z_0} + \frac{Z_0}{Z_S})\tan\phi_S\right\} \tag{5}$$

Using (5), the derivatives of ϕ_T with ϕ_s and Z_s that appear in the right-hand side member of (1) are found to be

$$\frac{d\phi_T}{d\phi_S} = -\frac{1}{M^{-1}\cdot\cos^2\phi_S + M\cdot\sin^2\phi_S} \tag{6}$$

and

$$\frac{d\phi_T}{dZ_S} = -\frac{1/2}{1+M^2\cdot\tan^2\phi_S}\cdot\tan\phi_S\cdot(\frac{1}{Z_0} - \frac{Z_0}{Z_S^2}) \tag{7}$$

respectively, where the dimensionless factor *M*, defined as follows

$$M = \frac{1}{2}(\frac{Z_S}{Z_0} + \frac{Z_0}{Z_S}) \tag{8}$$

is used for simplification purposes. The remaining two derivatives of the right-hand side member of (1) can be easily calculated. By considering sensor implementation in microstrip technology (the interest in this work), such terms are given by [73]

$$\frac{d\phi_S}{d\varepsilon_{MUT}} = \frac{\phi_S}{4\varepsilon_{eff}}(1-F) \tag{9}$$

and

$$\frac{dZ_S}{d\varepsilon_{MUT}} = -\frac{Z_S}{4\varepsilon_{eff}}(1-F) \tag{10}$$

where the effective dielectric constant is [81]

$$\varepsilon_{eff} = \frac{\varepsilon_r + \varepsilon_{MUT}}{2} + \frac{\varepsilon_r - \varepsilon_{MUT}}{2}F \tag{11}$$

In (11), ε_r is the dielectric constant of the substrate and *F* is a geometry factor given by

$$F = (1+12\frac{h}{W_S})^{-\frac{1}{2}} \tag{12a}$$

for $W_s/h \geq 1$, or by

$$F = (1+12\frac{h}{W_S})^{-\frac{1}{2}} + 0.04(1-\frac{W_S}{h})^2 \tag{12b}$$

for $W_s/h < 1$, where *h* and W_s are the substrate thickness and the width of the sensing line, respectively, and it is assumed that $t << h$, where *t* is the thickness of the metallic layer. Moreover, the validity of (11) is subjected to the semi-infinite MUT approximation. That is, the MUT must be thick enough in the vertical direction, so that the electromagnetic field generated by the line does not reach the MUT-air interface. Note that for CPW technology, and considering both a semi-infinite substrate and MUT, the effective permittivity is given by (11) with $F = 0$. Thus, it follows that potentially higher sensitivity can be achieved by implementing the sensors in CPW (the fringing fields are higher in a CPW, and therefore the MUT has major effect on the phase and impedance of the sensing line).

Inspection of expression (8) indicates that if $Z_s = Z_0$ (a condition that guarantees perfect matching for the line loaded with the REF MUT sample), $M = 1$, and, consequently, $d\phi_T/d\phi_s = 1$. Moreover, $d\phi_T/dZ_s = 0$ for $Z_s = Z_0$, as it can be inferred from (7). Thus, for uniform matched sensing lines, the sensitivity is simply

$$S = \frac{d\phi_S}{d\varepsilon_{MUT}} = \frac{\phi_S}{4\varepsilon_{eff}}(1-F) \tag{13}$$

and it increases proportionally with ϕ_s.

For $Z_s \neq Z_0$, the line is mismatched and part of the injected power is reflected back to the source, unless $\phi_s = n\cdot\pi$, n being an integer number. For $\phi_s = n\cdot\pi$, it follows that $d\phi_T/d\phi_s = M$ and $d\phi_T/dZ_s = 0$. Thus, the sensitivity is found to be

$$S = \frac{d\phi_T}{d\phi_S}\cdot\frac{d\phi_S}{d\varepsilon_{MUT}} = \frac{M\cdot n\pi}{4\varepsilon_{eff}}(1-F) \tag{14}$$

Thus, as compared to the sensitivity of the matched line (i.e., with $Z_s = Z_0$) with identical electrical length, the sensitivity is multiplied by a factor that depends on M, given by (8) (note that the geometry factor, F, is not identical in a matched and in a mismatched line, and, for this reason, the sensitivity is not exactly multiplied by M). Indeed, M increases either by increasing or decreasing the normalized impedance of the sensing line, Z_s/Z_0. However, a high line impedance is preferred since the width of the line, W_s, decreases by increasing Z_s, and this, in turn, reduces the geometry factor F, thereby boosting up the sensitivity.

Let us next consider the complete structure of Fig. 1. The *ABDC* matrix of the whole two-port network can be inferred from the product of the *ABCD* matrices of each line section. We do assume that the step-impedance discontinuities are ideal, and therefore not included in the schematic model of Fig 1(a), thereby avoiding an excessively complex formulation. Nevertheless, the main effects of such impedance variations are accounted for by the model, as inferred from the reasonable prediction of the sensitivities, as will be shown later. Introducing the resulting elements of the *ABCD* matrix in (2), the transmission coefficient can be easily inferred, and, from it, the phase is found to be

$$\phi_T = -\arctan\left\{\frac{(\frac{Z_S}{Z_0}+\frac{Z_0}{Z_S})\cos\phi\sin\phi_S + (\frac{Z}{Z_0}+\frac{Z_0}{Z})\sin\phi\cos\phi_S}{2\cos\phi\cos\phi_S - (\frac{Z}{Z_s}+\frac{Z_s}{Z})\sin\phi\sin\phi_S}\right\} \tag{15}$$

The sensitivity is also given by expression (1), where the terms (9) and (10) are valid, as well. Calculation of the derivatives $d\phi_T/d\phi_s$ and $d\phi_T/dZ_s$ from (15) gives

$$\frac{d\phi_T}{d\phi_S} = -\frac{1}{1+(\frac{N}{D})^2}\cdot\frac{D\cdot N_{\phi_S}' - N\cdot D_{\phi_S}'}{D^2} \tag{16}$$

$$\frac{d\phi_T}{dZ_S} = -\frac{1}{1+(\frac{N}{D})^2}\cdot\frac{D\cdot N_{Z_S}' - N\cdot D_{Z_S}'}{D^2} \tag{17}$$

where N and D are the numerator and the denominator, respectively, of the argument of the arctan in (15), and the following derivatives have been defined

$$N_{\phi_S}' \equiv \frac{dN}{d\phi_S} = (\frac{Z_S}{Z_0}+\frac{Z_0}{Z_S})\cos\phi\cos\phi_S - (\frac{Z}{Z_0}+\frac{Z_0}{Z})\sin\phi\sin\phi_S \tag{18}$$

$$D_{\phi_S}' \equiv \frac{dD}{d\phi_S} = -2\cos\phi\sin\phi_S - (\frac{Z}{Z_S}+\frac{Z_S}{Z})\sin\phi\cos\phi_S \tag{19}$$

$$N_{Z_S}' \equiv \frac{dN}{dZ_S} = (\frac{1}{Z_0}-\frac{Z_0}{Z_S^2})\cos\phi\sin\phi_S \tag{20}$$

$$D_{Z_S}' \equiv \frac{dD}{dZ_S} = (\frac{Z}{Z_S^2}-\frac{1}{Z})\sin\phi\sin\phi_S \tag{21}$$

In order to ensure the absence of mismatching reflections it is necessary that either $Z_s = Z = Z_0$, or $Z_s = Z \neq Z_0$ with $\phi + \phi_s = n\cdot\pi$. In the former case, the sensitivity is also given by (13), and this trivial case lacks interest. In the second case ($Z_s = Z \neq Z_0$), (16) and (17) are found to be

$$\frac{d\phi_T}{d\phi_S} = -\frac{1}{M^{-1}\cdot\cos^2(\phi+\phi_S)+M\cdot\sin^2(\phi+\phi_S)} \tag{22}$$

and

$$\frac{d\phi_T}{dZ_S} = -\frac{1}{Z_S}\cdot\frac{\cos(\phi+\phi_S)\cdot\cos\phi\sin\phi_S\cdot\frac{Z_S^2-Z_0^2}{Z_S^2+Z_0^2}}{M^{-1}\cdot\cos^2(\phi+\phi_S)+M\cdot\sin^2(\phi+\phi_S)} \tag{23}$$

respectively, and using $\phi + \phi_s = n\cdot\pi$ one obtains

$$\frac{d\phi_T}{d\phi_S} = -M \tag{24}$$

and

$$\frac{d\phi_T}{dZ_S} = -(-1)^n\cdot\frac{M}{Z_S}\cdot\cos(n\cdot\pi-\phi_S)\sin\phi_S\cdot\frac{Z_S^2-Z_0^2}{Z_S^2+Z_0^2} \tag{25}$$

where (25) is null if $\phi = (2m + 1)\cdot\pi/2$ [and consequently $\phi_s = (2n - 2m - 1)\cdot\pi/2$] or $\phi_s = m\cdot\pi$ (and consequently $\phi = (n - m)\cdot\pi$), where m is an integer satisfying $m < n$. If (25) is null, the sensitivity is given by (14), and, obviously, the phase combination $\phi_s = m\cdot\pi$ and $\phi = (n - m)\cdot\pi$ provides a better sensitivity (note that this case is, indeed, the one where the line section with impedance Z and phase ϕ is absent). Nevertheless, the optimum values of the phases of the lines (which should satisfy $\phi + \phi_s = n\cdot\pi$ for matching requirements) are those that maximize the whole sensitivity, which can be expressed as

$$S = \frac{d\phi_T}{d\varepsilon_{MUT}} = -\frac{M(1-F)}{4\varepsilon_{eff}}\left\{\phi_S - (-1)^n\cdot\cos(n\cdot\pi-\phi_S)\sin\phi_S\cdot\frac{Z_S^2-Z_0^2}{Z_S^2+Z_0^2}\right\} \tag{26}$$

In order to find the optimum value of ϕ_s, the derivative of (26) with regard to ϕ_s is obtained, i.e.,

$$\frac{dS}{d\phi_S} = -\frac{M(1-F)}{4\varepsilon_{eff}}\left\{1-\frac{Z_S^2-Z_0^2}{Z_S^2+Z_0^2}\cdot\cos(2\phi_S)\right\} \tag{27}$$

and by forcing it to be zero, one obtains

$$\cos(2\phi_S) = \frac{Z_S^2+Z_0^2}{Z_S^2-Z_0^2} \tag{28}$$

Since there are not real solutions of (28) for ϕ_s, it follows that the sensitivity does not exhibit a maximum (or a minimum). Indeed, the magnitude of the sensitivity monotonically increases with ϕ_s, as it can be appreciated in Fig. 2. Thus, the optimum phase values are those satisfying $\phi_s = m\cdot\pi$ (and thereby $\phi = (n - m)\cdot\pi$), and the sensitivity is given by expression (14). Naturally, for sensor size optimization, the line with impedance Z and phase $\phi = (n - m)\cdot\pi$ can be excluded from the design (corresponding to $n = m$), and the sensor is indeed the one analyzed in the previous case. However, this result was not a priori evident, but derived from the detailed analysis carried out in this section. The main conclusion is that the sensing line must be chosen to exhibit a phase of $\phi_s = m\cdot\pi$, i.e., a half-wavelength or a multiple of it, when it is loaded with the REF MUT, and the characteristic impedance must be as high as possible. The phase condition $\phi_s = m\cdot\pi$ prevents from mismatching reflections, whereas the high value of the characteristic impedance of the sensing line section increases the sensitivity.

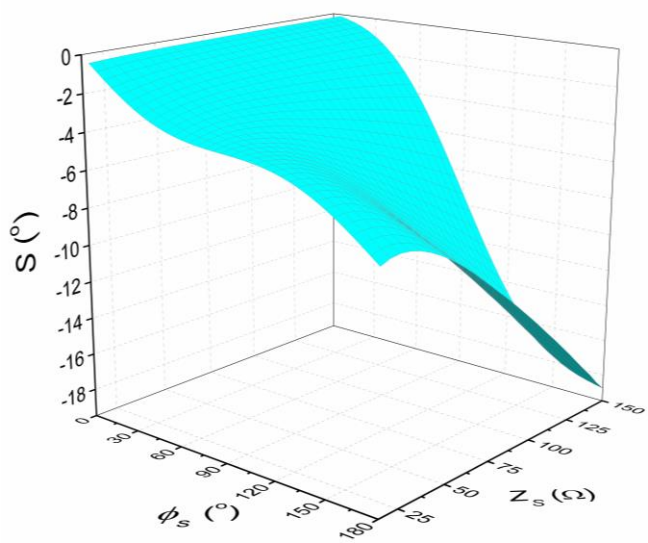

Fig. 2. Representation of the sensitivity, as given by (26), as a function of ϕ_s for n = 1, and for different values of Z_s. For the evaluation of F and ε_{eff}, the parameters of the *Rogers 4003C* substrate, with thickness h = 1.524 mm and dielectric constant ε_r = 3.55, have been used.

IV. SENSOR DESIGN, FABRICATION, AND VALIDATION

For validation purposes, three different sensors have been designed and fabricated. All the sensors verify that the electrical lengths satisfy the matching requirement, i.e., $\phi + \phi_s = n\cdot\pi$. In sensor A, $\phi = 0$, $\phi_s = \pi$, and $Z_s = Z_0 = 50\ \Omega$, when the REF MUT is a piece of the uncladded *Rogers 4003C* substrate with dielectric constant ε_r = 3.55 and thickness h = 4.572 mm (achieved by stacking 3 samples). In sensor B, $\phi = 0$, $\phi_s = \pi$, and $Z_s = 124\ \Omega$, with the same REF MUT. Finally, in sensor C, part of the half-wavelength line is not covered by the MUT, specifically, $\phi = \pi/4$, $\phi_s = 3\pi/4$, and the impedances are set to $Z = Z_s = 124\Omega$. The operating frequency in all the sensors is f_0 = 2 GHz. It should be mentioned that for sensor C the width of the line sections is different, despite the fact that the impedances are identical. The reason is that the $3\pi/4$ sensing line should exhibit the design impedance, $Z_s = 124\Omega$, when it is loaded with the REF MUT (the one indicated above), whereas the $\pi/4$ line should exhibit an identical impedance ($Z = 124\Omega$) when it is surrounded by air. The sensors have been implemented on the *Rogers 4003C* substrate with thickness h = 1.524 mm, dielectric constant ε_r = 3.55, and loss tangent tanδ = 0.0022.

With the indicated substrate, REF MUT, phases, and impedances, the line dimensions have been calculated, and then the prototype sensors have been fabricated by means of a *LPKF H100* drilling machine. The photographs, as well as the relevant dimensions, of the fabricated sensors are depicted in Fig. 3. Note that identical access lines have been added to the half-wavelength sensor lines for connector soldering.

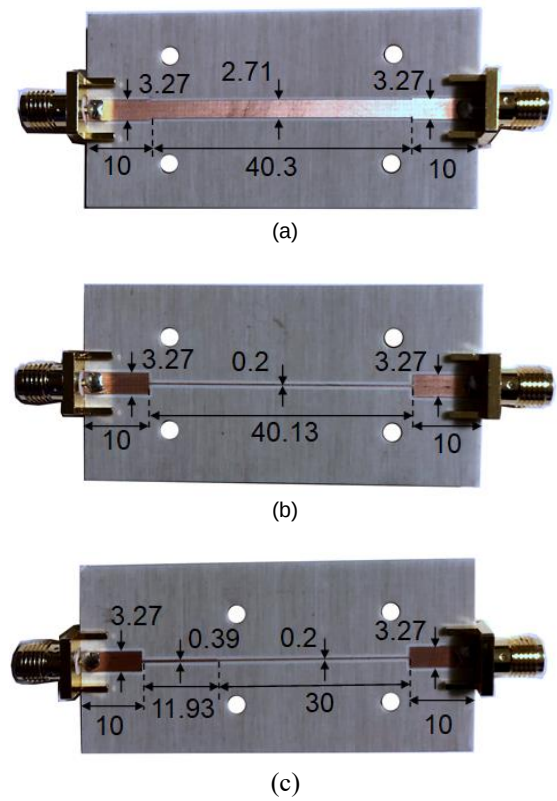

Fig. 3. Photographs of the fabricated sensors and relevant dimensions (in mm). (a) Sensor A; (b) Sensor B; (c) Sensor C. The sensing regions are given by the (imaginary) rectangles with vertexes corresponding to the positions of the holes, which are used for screwing the samples against the sensing line section, thereby minimizing the effects of the air gap.

Prior to measurements, the dependence of the phase of the transmission coefficient with the dielectric constant of the MUT for the three sensors has been obtained by means of electromagnetic simulation, using the *CST Microwave Studio* commercial software. The considered input dynamic range is $1 < \varepsilon_{MUT} < 10.2$, limited by the dielectric constant of air and the dielectric constant of a *Rogers RO3010* substrate available in our laboratory. The results are depicted in Fig. 4 (a), where the phase of the transmission coefficient is actually represented in

reference to the phase of the transmission coefficient when the REF MUT is on top of the sensing region. Actually, the simulation results of Fig. 4(a) were repeated by considering values of the loss tangent of the MUT of 0.0025, 0.0050 and 0.0100, and the results (not shown) are indistinguishable. The measured phases of the transmission coefficient for specific MUT samples, with the dielectric constants indicated in the caption of Fig. 4, are also depicted in the figure (such phases have been inferred by means of the vector network analyzer *Keysight N5221A*, see Fig. 5). As it can be seen, there is very good agreement between the simulated and the measured data points.

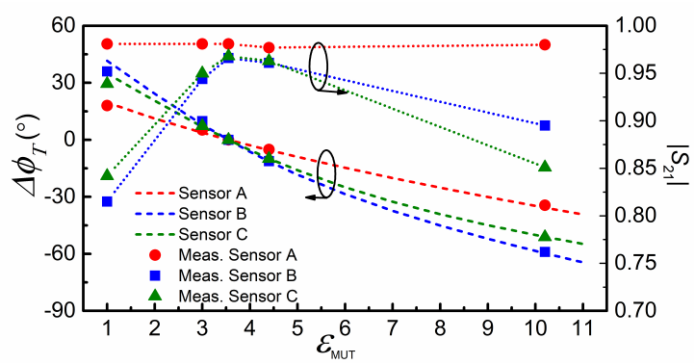

(a)

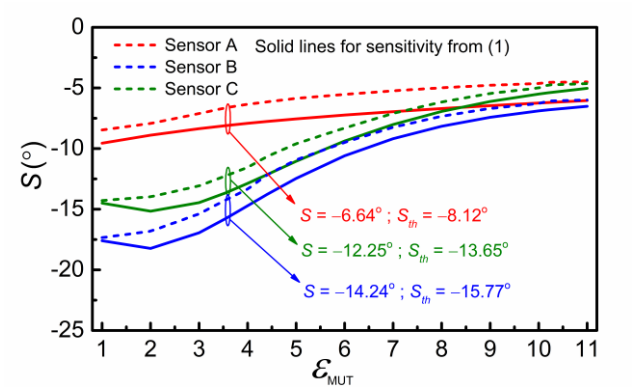

(b)

Fig. 4. Measured and simulated phase of the transmission coefficient at the operating frequency for the sensors of Fig. 3 (a), and simulated sensitivity (b). The considered MUTs for measurements are 4.57-mm slabs of uncoated *PLA* (ε_{MUT} = 3), *Rogers RO4003C* (ε_{MUT} = 3.55), *FR4* (ε_{MUT} = 4.4) and *Rogers RO3010* (ε_{MUT} = 10.2) substrates. In (a), the measured magnitude of the transmission coefficient at the operating frequency for the considered MUT samples is also included.

Due to the lack of a numerous set of experimental data points, the sensitivity has been inferred from the derivative of the simulated data. The results are depicted in Fig. 4(b). The figure provides the value of the sensitivity for the REF MUT that results from the simulated data points, as well as the one inferred by means of expression (26), and designated as S_{th}. As it can be appreciated, the agreement is reasonably good for all three sensors, pointing out the validity of the sensitivity analysis carried out in the previous section. Indeed, Fig. 4(b) includes also the sensitivity as a function of ε_{MUT}, inferred theoretically by means of expression (1), with the different derivative terms calculated according to (9), (10), (16) and (17). Note that (22) and (23) are only valid for $Z = Z_s$, which is satisfied when $\varepsilon_{MUT} = \varepsilon_{REF}$, and expressions (24) and (25) need that the phases satisfy $\phi + \phi_s = n \cdot \pi$, a condition fulfilled when $\varepsilon_{MUT} = \varepsilon_{REF}$, as well. Obviously, for the calculation of the theoretical sensitivity over the input dynamic range, it is necessary to previously obtain the involved line phases and impedances for each value of ε_{MUT}.

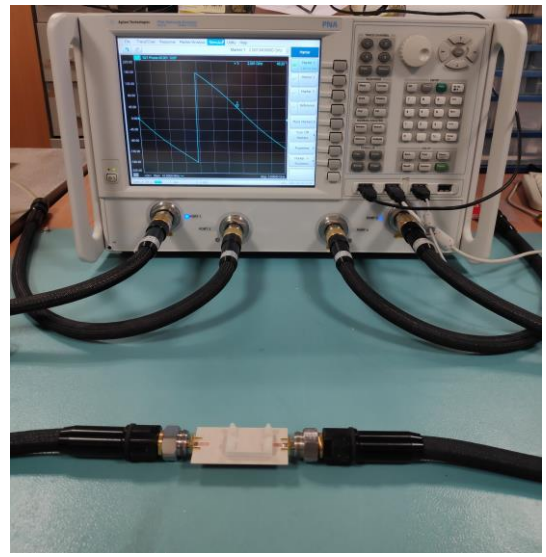

Fig. 5. Photograph of the experimental setup used for the phase measurements, including the vector network analyzer *Keysight N5221A* and the sensor with a MUT on top of the sensing region.

As it can be seen from Fig 4(b), the agreement between the theoretical and simulated sensitivity is reasonably good within the whole considered range. This further strengths the validity of the theoretical analysis of Section III. The slight discrepancies between the results predicted by the theory and those inferred from the electromagnetic simulations are attributed to non-idealities, such as the limited thickness of the considered MUTs (not semi-infinite in practice), and to the fact that the calculation of Z_s and ϕ_s with a certain MUT on top of the sensing line section is subjected to some inaccuracies.

It should be mentioned that the proposed sensors are especially suited for applications where accurate measurements of the dielectric constant of the MUT in the vicinity of that of the REF MUT sample, or a related material magnitude, are required. Thus, the present study reports a method to optimize the sensitivity, for a given reference sample, in a kind of sensors where design simplicity and size are key aspects. We would like to clarify that the fact that the sensitivity is optimized for a given value of the dielectric constant of the MUT (the REF MUT) does not necessarily mean that the maximum magnitude of the sensitivity over the considered input dynamic is the one corresponding to such value of the dielectric constant of the MUT (ε_{REF}). As it can be seen in Fig. 4, the maximum value of the magnitude of the sensitivity actually takes place for $\varepsilon_{MUT} = 1$ (simulated values) in the three designed and fabricated sensors. In the sensors reported in [73], the maximum magnitude of the sensitivity for the considered input dynamic range was also

found to occur at $\varepsilon_{MUT} = 1$, but the sensitivity in such sensors was optimized for this value of the dielectric constant of the MUT (i.e., $\varepsilon_{REF} = 1$). By contrast, in the sensors reported in [76], the magnitude of the sensitivity is a maximum for a dielectric constant value of roughly 3.55, the value of ε_{REF}.

As expected, the results of Fig. 4 confirm that the optimum sensitivity in the limit when $\varepsilon_{MUT} \rightarrow \varepsilon_{REF}$ is achieved for Sensor B, the one where the entire half-wavelength line, with significant impedance contrast ($Z_s/Z_0 = 2.48$), acts as sensing line. The worst sensitivity corresponds to sensor A, based on a half-wavelength matched line (with $Z_s = Z_0 = 50\ \Omega$). Increasing Z_s enhances the sensitivity. Concerning the limit of such impedance, it is dictated by the minimum width of the line that can be achieved with the technology in use, typically around 200 μm with most drilling machines (this is the case of the sensing line width in sensor B). Nevertheless, it is possible to increase the sensitivity by adding further 180º sensing line sections to the sensor (at the expense, of course, of increasing the size of the sensing region).

Concerning resolution, it is defined as the minimum input variable (in our case the dielectric constant) that can be resolved. Obviously, resolution is intimately related to the sensitivity. Thus, if we consider that the phase resolution (output variable) is of the order of 5º, a very conservative value, the resolution for discriminating variations in the dielectric constant of the MUT with regard to the one of the REF sample is roughly $\Delta\varepsilon_{MUT} = 0.35$. Obviously, such resolution can be improved (reduced) by enhancing the sensitivity by adding further 180º line sections to the sensing line.

A figure of merit (*FoM*) in phase-variation sensors is the ratio between the maximum sensitivity and the size of the sensing region expressed in terms of the squared guided wavelength, λ. Table I contains the *FoM*, as well as other sensor parameters, for the three sensors designed and fabricated in this work, and for other phase-variation dielectric constant sensors available in the literature and operating in transmission. Actually, for the calculation of the *FoM* in the sensors of this work, the value of the sensitivity for $\varepsilon_{REF} = 3.55$, rather than the maximum sensitivity, has been considered. Also, for the calculation of the size of the sensing region, a width of 0.1 λ has been considered for the sensors of this work. This value is very conservative, which means that the *FoM* is indeed underestimated (note that with such width, it is by far guaranteed that the electric field lines generated by the line do not extend beyond the MUT boundaries, a necessary condition).

As it can be seen from Table I, sensors B and C are competitive in terms of the *FoM* (though sensor B exhibits better sensitivity). Moreover, in sensor B, except by the access lines and connectors, the whole sensor is the sensing region, thereby corresponding to an optimized design. The sensitivity in sensor [70] is very high, but at the expense of a significantly large sensing area. By contrast, any of the designed and fabricated sensors of this paper is very small, as far as the whole sensor (obviously excluding the associated electronics) merely consists of a half-wavelength line section, the sensitive part being the whole line (Sensors A and B) or a fraction of it (Sensor C). Obviously, the sensitivity of Sensors A, B and C can be further enhanced by considering additional half-wavelength line sections.

In the sensor reported in [78], the sensitivity and the *FoM* are very competitive. In such sensor, a slow-wave transmission line based on a host line periodic loaded with patch capacitors is used for sensing (the sensitive elements are the patch capacitances). These slow-wave transmission line based sensors exhibit good performance, but their design is not exempt of certain complexity, at least as compared to the sensors reported in this paper. Indeed, the characteristic (or Bloch) impedance of the sensor in [78] is 50 Ω, whereas the phase is not subjected to a specific value. Namely, impedance matching is considered in [78], contrary to the sensor proposed in this paper, where phase matching is forced (i.e., the sensing line is a half-wavelength line when it is loaded with the REF sample). However, it is possible to apply phase matching to the sensors of [78], by considering a slow-wave transmission line with a phase of 180º, or multiple of it, and high value of the Bloch impedance, with potential sensitivity enhancement. Nevertheless, this aspect requires further investigation and is left for a future work.

It should be mentioned that in some of the sensors in Table I ([45],[53],[54]), the phase information was transformed to magnitude information. For this reason, the sensitivity in these sensors is given in dB, in coherence with the output variable, i.e., the magnitude of the transmission coefficient. The sensors reported in [45],[53], are based on artificial transmission lines (i.e., composite right left/handed lines in [45], and electro-inductive-wave transmission lines in [53]). Such lines exhibit significant (and controllable) dispersion, useful to enhance the sensitivity, but, similar to those sensors based on slow-wave transmission lines [77],[78], the design of sensors based on artificial lines is not straightforward.

TABLE I
COMPARISON OF VARIOUS TRANSMISSION-MODE PHASE-VARIATION SENSORS

Ref.	*Mode*	*Size* (λ^2)	*Max. Sensitivity*	*FoM* (º/λ^2)
[45]	TRANSMISSION	---	600 dB	---
[69]	TRANSMISSION	---	54.8º	---
[70]	TRANSMISSION	12.90	415.6º	32.2
[53]	TRANSMISSION	0.075	25.3 dB	---
[54]	TRANSMISSION	0.020	17.6 dB	---
[77]	TRANSMISSION	0.030	7.7º	257
[78]	TRANSMISSION	0.040	20.0º	500
Sensor A	TRANSMISSION	0.050	6.64º	132.8
Sensor B	TRANSMISSION	0.050	14.24º	284.8
Sensor C	TRANSMISSION	0.038	12.25º	322.4

We would also like to mention that the reflective-mode phase-variation sensors reported in [73],[74] are very competitive in terms of sensitivity and *FoM*. However, measuring the phase of a transmission coefficient in a real scenario, that is, avoiding the use of a VNA, seems to be more feasible than measuring the phase of the reflection coefficient. This is the main advantage of the reported sensor, as compared to the sensors reported in [73],[74].

Finally, let us indicate that the loss tangent of solids samples with moderate- and low-loss factors cannot be accurately estimated with this approach. Nevertheless, the reported

sensors are useful to measure other variables related to the dielectric constant, e.g., material composition, or to detect defects in samples, typically manifested by a variation in the effective dielectric constant. In general, resonant methods [24]-[28],[82]-[84] offer a good option to estimate the loss tangent with reasonable accuracy. However, the proposed sensors, or more generally, phase-variation sensors, are interesting because the sensitivity can be enhanced by means of specific methods, like the one reported in this work, or by simply elongating the sensing line.

V. CONCLUSIONS

In conclusion, it has been demonstrated that the sensitivity in transmission-line-based phase-variation permittivity sensors operating in transmission can be enhanced through impedance contrast, and by setting the length of the sensing line to a half-wavelength (or a multiple of this length) at the operating frequency. In particular, in one of the designed and fabricated prototype sensors, implemented in microstrip technology, the sensitivity for small perturbations has been found to be 2.1 times larger than the one of the sensors based on an ordinary matched (50-Ω) half-wavelength sensing line. This sensitivity optimization has not been only demonstrated by simulation and experiment, but also through a detailed analysis of the structure, useful to predict the value of the sensitivity. The proposed sensors are very simple and small, since the sensing part merely consists of a half-wavelength transmission line. This facilitates sensor design and fabrication, and provides robustness against fabrication related tolerances (more critical in designs involving metallic or slotted resonant elements, or other complex structures, such as artificial lines, etc.). The fact that the sensors operate at a single frequency, and that the phase, the output variable, is robust against the pernicious effects of electromagnetic interference and noise are additional advantageous aspects of the reported sensors.

REFERENCES

[1] T. W. Athey, M. A. Stuchly, and S. S. Stuchly, "Measurement of radio frequency permittivity of biological tissues with an open-ended coaxial line: part I," *IEEE Trans. Microw. Theory Techn*. vol. 30, pp. 82–86, 1982.

[2] J. P. Grant, R. N. Clarke, G. T. Symm, and N. M. Spyron, "A Critical study of the open-ended coaxial-line sensor technique for RF and microwave complex permittivity measurements," *J. Phys. E Sci. Instrum*. vol. 22, pp. 757–770, 1989.

[3] D. Misra, "On the measurement of the complex permittivity of materials by an open-ended coaxial probe," *IEEE Microw. Guid. Wave Lett.*, vol. 5, pp. 161–163, 1995.

[4] A. La Gioia, E. Porter, I. Merunka, A. Shahzad, S. Salahuddin, M. Jones, and M. O'Halloran, "Open-ended coaxial probe technique for dielectric measurement of biological tissues: challenges and common practices," *Diagnostics*, vol. 8, paper 40, 2018.

[5] A. Gregory, R. Clarke, "A Review of RF and microwave techniques for dielectric measurements on polar liquids," *IEEE Trans. Dielectr. Electr. Insul*., vol. 13, pp. 727–743, 2006.

[6] Agilent. *Basics of Measuring the Dielectric Properties of Materials*; Agilent Technologies: Santa Clara, CA, USA, 2005.

[7] D. V. Land, and A. M. Campbell, "A quick accurate method for measuring the microwave dielectric properties of small tissue samples," *Phys. Med. Biol*., vol. 37, p. 183, 1992.

[8] A. Campbell, and D. V. Land, "Dielectric properties of female human breast tissue measured in vitro at 3.2 GHz," *Phys. Med. Biol*., vol. 37, pp. 193–210, 1992.

[9] Z. Peng, J. Y. Hwang, and M. Andriese, "Maximum sample volume for permittivity measurements by cavity perturbation technique," *IEEE Trans. Instrum. Meas*., vol. 63, pp. 450–455, 2014.

[10] A. Campbell, "Measurements and analysis of the microwave dielectric properties of tissues," *J. Appl. Phys*., vol. 22, p. 95, 1990.

[11] P. Wei, B. Morey, T. Dyson, N. McMahon, Y. Y. Hsu, S. Gazman, L Klinker, B. Ives, K. Dowling, and C. Rafferty, "A conformal sensor for wireless sweat level monitoring," *IEEE Sensors*, Baltimore, MD, USA, 2013.

[12] L. Su, X. Huang, W. Guo and H. Wu, "A flexible microwave sensor based on complementary spiral resonator for material dielectric characterization," *IEEE Sensors J*., vol. 20, no. 4, pp. 1893-1903, Feb. 2020.

[13] K. Grenier, D. Dubuc, P. E. Poleni, M. Kumemura, H. Toshiyoshi,T. Fujii, and H. Fujita, "Integrated broadband microwave and microfluidic sensor dedicated to bioengineering," *IEEE Trans. Microw. Theory Techn.*, vol. 57(12), pp. 3246-3253, 2009.

[14] T. Chretiennot, D. Dubuc, and K. Grenier, "A microwave and microfluidic planar resonator for efficient and accurate complex permittivity characterization of aqueous solutions," *IEEE Trans. Microw. Theory Techn.*, vol. 61(2), pp. 972-978, 2012.

[15] A. Salim, S. H. Kim, J. Y. Park, and S. Lim, "Microfluidic biosensor based on microwave substrate-integrated waveguide cavity resonator," *J. Sensors*, vol. 2018, Article ID 1324145, 2018.

[16] M. H. Zarifi, H. Sadabadi, S. H. Hejazi, M. Daneshmand, and A. Sanati-Nezhad, "Noncontact and nonintrusive microwave-microfluidic flow sensor for energy and biomedical engineering," *Sci. Rep*., vol. 8(1), p. 139, 2018.

[17] M. M. Rodgers, V. M. Pai, and R. S. Conroy, "Recent advances in wearable sensors for health monitoring," *IEEE Sensors J*., vol. 15(6), pp. 3119-3126, 2014.

[18] J. Castillo-León, W. E. Svendsen, *Lab-on-a-Chip Devices and Micro-Total Analysis Systems*, Springer, New York, NY, USA, 2015.

[19] Y. S. Zhang, "Modular multi-organ-on-chips platform with physicochemical sensor integration," in *2017 IEEE 60th International Midwest Symposium on Circuits and Systems* (MWSCAS), Boston, MA, 2017, pp. 80-83.

[20] A. T. Singh, D. Lantigua, A. Meka, S. Taing, M. Pandher, and G. Camci-Unal, "Paper-based sensors: emerging themes and applications," *Sensors*, vol. 18, pp. 2838, 2018.

[21] M. Puentes, C. Weiß, M. Schüßler, and R. Jakoby, "Sensor array based on split ring resonators for analysis of organic tissues," in *IEEE MTT-S Int. Microw. Symp.*, Baltimore, MD, USA, Jun. 2011, pp. 1−4.

[22] A. Ebrahimi, W. Withayachumnankul, S. Al-Sarawi, and D. Abbott, "High-sensitivity metamaterial-inspired sensor for microfluidic dielectric characterization," *IEEE Sensors J.*, vol. 14, no. 5, pp. 1345−1351, May 2014

[23] M. Schüßler, C. Mandel, M. Puentes, and R. Jakoby, "Metamaterial inspired microwave sensors," *IEEE Microw. Mag.*, vol. 13, no. 2, pp. 57–68, Mar. 2012.

[24] M. S. Boybay and O. M. Ramahi, "Material characterization using complementary split-ring resonators," *IEEE Trans. Instrum. Meas*., vol. 61, no. 11, pp. 3039−3046, Nov. 2012.

[25] C.-S. Lee and C.-L. Yang, "Complementary split-ring resonators for measuring dielectric constants and loss tangents," *IEEE Microw. Wireless Compon. Lett.*, vol. 24, no. 8, pp. 563−565, Aug. 2014.

[26] C.-L. Yang, C.-S. Lee, K.-W. Chen, and K.-Z. Chen, "Noncontact measurement of complex permittivity and thickness by using planar resonators," *IEEE Trans. Microw. Theory Techn.*, vol. 64, no.1, pp. 247−257, Jan. 2016.

[27] L. Su, J. Mata-Contreras, P. Vélez, and F. Martín, "Estimation of the complex permittivity of liquids by means of complementary split ring resonator (CSRR) loaded transmission lines," in *2017 IEEE MTT-S International Microwave Workshop Series on Advanced Materials and Processes* (IMWS-AMP 2017), Pavia, Italy, 20-22 Sep. 2017.

[28] L. Su, J. Mata-Contreras, P. Vélez, A. Fernández-Prieto, and F. Martín, "Analytical method to estimate the complex permittivity of oil Samples," *Sensors*, 18(4), paper 984, 2018.

[29] A.K, Jha, N, Delmonte, A, Lamecki, M, Mrozowski, and M, Bozzi, "Design of microwave-based angular displacement sensor," *IEEE Microw. Wireless Compon. Lett.*, vol. 29 (4), pp. 306-308, Apr. 2019.

[30] G. Galindo-Romera, F. J. Herraiz-Martínez, M. Gil, J. J. Martínez-Martínez, and D. Segovia-Vargas, "Submersible printed split-ring resonator-based sensor for thin-film detection and permittivity

characterization," *IEEE Sensors J*., vol. 16, no. 10, pp. 3587-3596, May, 2016.

[31] R. A. Alahnomi, Z. Zakaria, E. Ruslan, S. R. A. Rashid, and A. A. M. Bahar, "High-Q sensor based on symmetrical split ring resonator with spurlines for solids material detection," *IEEE Sens. J.*., vol. 17, no. 9, pp. 2766-2775, May 2017.

[32] N. Jankovic and V. Radonic "A Microwave Microfluidic Sensor Based on a Dual-Mode Resonator for Dual-Sensing Applications," *Sensors*, vol. 17(12), p. 2713, 2017.

[33] H. Zhou, D. Hu, C. Yang, C. Chen, J. Ji, M. Chen, Y. Chen, Y. Chen, Y. Yang, and X. Mu, "Multi-Band Sensing for Dielectric Property of Chemicals Using Metamaterial Integrated Microfluidic Sensor," *Sci. Rep.*, vol. 8, paper 14801, 2018.

[34] M. A. H. Ansari, A. K. Jha, Z. Akhter, and M. J. Akhtar, "Multi-band RF planar sensor using complementary split ring resonator for testing of dielectric materials," *IEEE Sensors J*., vol. 18, no. 16, pp. 6596-6606, Aug. 2018.

[35] H. Lobato-Morales, J. H. Choi, H. Lee, and J. L. Medina-Monroy, "Compact dielectric-permittivity sensors of liquid samples based on substrate-integrated-waveguide with negative-order-resonance," *IEEE Sensors J*., vol. 19, no. 19, pp. 8694-8699, Oct. 2019.

[36] Y. Khanna and Y.K Awasthi, "Dual-band microwave sensor for investigation of liquid impurity concentration using a metamaterial complementary split-ring resonator," *J. Elect. Mat*., vol 49, pp. 385–394, 2020.

[37] A. K. Horestani, J. Naqui, Z. Shaterian, D. Abbott, C. Fumeaux, and F. Martín, "Two-dimensional alignment and displacement sensor based on movable broadside-coupled split ring resonators," *Sensors and Actuators A*, vol. 210, pp. 18–24, Apr. 2014.

[38] J. Naqui, C. Damm, A. Wiens, R. Jakoby, L. Su, and F. Martín, "Transmission lines loaded with pairs of magnetically coupled stepped impedance resonators (SIRs): modeling and application to microwave sensors," in *IEEE MTT-S Int. Microwave Symp*., Tampa, FL, USA, Jun. 2014, pp. 1–4.

[39] L. Su, J. Naqui, J. Mata-Contreras, and F. Martín, "Modeling metamaterial transmission lines loaded with pairs of coupled split ring resonators," *IEEE Ant. Wireless Propag. Lett.*, vol. 14, pp. 68–71, 2015.

[40] L. Su, J. Naqui, J. Mata-Contreras, and F. Martín, "Modeling and applications of metamaterial transmission lines loaded with pairs of coupled complementary split ring resonators (CSRRs)," *IEEE Ant. Wireless Propag. Lett.*, vol. 15, pp. 154–157, 2016.

[41] L. Su, J. Mata-Contreras, J. Naqui, and F. Martín, "Splitter/combiner microstrip sections loaded with pairs of complementary split ring resonators (CSRRs): modeling and optimization for differential sensing applications," *IEEE Trans. Microw. Theory Techn*., vol. 64, pp. 4362-4370, Dec. 2016.

[42] J. Naqui, C. Damm, A. Wiens, R. Jakoby, L. Su, J. Mata-Contreras, and F. Martín, "Transmission lines loaded with pairs of stepped impedance resonators: modeling and application to differential permittivity measurements," *IEEE Trans. Microw. Theory Techn.*, vol. 64, no. 11, pp. 3864-3877, Nov. 2016.

[43] A. Ebrahimi, J. Scott, and K. Ghorbani, "Differential sensors using microstrip lines loaded with two split ring resonators," *IEEE Sensors J.*, vol. 18, pp. 5786-5793, Jul. 2018.

[44] P. Vélez, L. Su, K. Grenier, J. Mata-Contreras, D. Dubuc, and F. Martín, "Microwave microfluidic sensor based on a microstrip splitter/combiner configuration and split ring resonators (SRR) for dielectric characterization of liquids", *IEEE Sensors J.*, vol. 17, pp. 6589-6598, Oct. 2017.

[45] C. Damm, M. Schussler, M. Puentes, H. Maune, M. Maasch, and R. Jakoby, "Artificial transmission lines for high sensitive microwave sensors," in *IEEE Sensors Conf.*, Christchurch, New Zealand, pp.755−758, Oct. 2009.

[46] J. Muñoz-Enano, P. Vélez, M. Gil, and F. Martín, "Planar microwave resonant sensors: a review and recent developments", *Appl. Sci*., vol. 10, p. 2615 (29 pages), 2020; doi:10.3390/app10072615.

[47] P. Vélez, J. Mata-Contreras, L. Su, D. Dubuc, K. Grenier, and F. Martín, "Modeling and analysis of pairs of open complementary split ring resonators (OCSRRs) for differential permittivity sensing," in *2017 IEEE MTT-S International Microwave Workshop Series on Advanced Materials and Processes* (IMWS-AMP 2017), Pavia, Italy, 20-22 September 2017.

[48] P. Vélez, K. Grenier, J. Mata-Contreras, D. Dubuc, and F. Martín, "Highly-sensitive microwave sensors based on open complementary split ring resonators (OCSRRs) for dielectric characterization and solute concentration measurement in liquids," *IEEE Access*, vol. 6, pp. 48324-48338, Aug. 2018.

[49] A. Ebrahimi, J. Scott, and K. Ghorbani, "Transmission lines terminated with LC resonators for differential permittivity sensing," *IEEE Microw. Wireless Compon. Lett*., vol. 28(12), pp. 1149-1151, Dec. 2018.

[50] P. Vélez, J. Muñoz-Enano, K. Grenier, J. Mata-Contreras, D. Dubuc, and F. Martín, "Split ring resonator (SRR) based microwave fluidic sensor for electrolyte concentration measurements," *IEEE Sensors J.*, vol. 19, no. 7, pp. 2562-2569, Apr. 2019.

[51] P. Vélez, J. Muñoz-Enano, M. Gil, J. Mata-Contreras, and F. Martín, "Differential microfluidic sensors based on dumbbell-shaped defect ground structures in microstrip technology: analysis, optimization, and applications," *Sensors*, vol. 19, page 3189, 2019.

[52] P. Vélez, J. Muñoz-Enano, and F. Martín, "Differential sensing based on quasi-microstrip-mode to slot-mode conversion," *IEEE Microw. Wireless Compon. Lett*., vol. 29, pp. 690-692, Oct. 2019.

[53] M. Gil, P. Vélez, F. Aznar-Ballesta, J. Muñoz-Enano, and F. Martín, "Differential sensor based on electro-inductive wave (EIW) transmission lines for dielectric constant measurements and defect detection," *IEEE Trans. Ant. Propag*., vol. 68, no. 3, pp. 1876-1886, Mar. 2020.

[54] J. Muñoz-Enano, P. Vélez, M. Gil, J. Mata-Contreras, and F. Martín, "Differential-mode to common-mode conversion detector based on rat-race couplers: analysis and application to microwave sensors and comparators," *IEEE Trans. Microw. Theory Techn*., vol. 68, pp. 1312-1325, Apr. 2020.

[55] J. Muñoz-Enano, P. Vélez, M. Gil, and F. Martín, "Microfluidic reflective-mode differential sensor based on open split ring resonators (OSRRs)," *Int. J. Microw. Wireless Technol*, vol. 12, pp. 588-597, Sep. 2020.

[56] J. Muñoz-Enano, P. Vélez, M. Gil, E. J. Cunilleras, A. Bassols, and F. Martín, "Characterization of electrolyte content in urine samples through a differential microfluidic sensor based on dumbbell-shaped defect ground structures," *Int. J. Microw. Wireless Technol*., vol. 12(9), pp. 817-824, Sep. 2020.

[57] A. Ebrahimi, F. J. Tovar-Lopez, J. Scott, and K. Ghorbani, "Differential microwave sensor for characterization of glycerol–water solutions," *Sens. & Act. B: Chem.*, vol. 321, Art. no. 128561, 2020.

[58] J. Naqui, M. Durán-Sindreu, and F. Martín, "Novel sensors based on the symmetry properties of split ring resonators (SRRs)," *Sensors*, vol 11, pp. 7545−7553, 2011.

[59] J. Naqui, M. Durán-Sindreu, and F. Martín, "Alignment and position sensors based on split ring resonators," *Sensors*, vol. 12, pp. 11790−11797, 2012.

[60] A. K. Horestani, C. Fumeaux, S.F. Al-Sarawi, and D. Abbott, "Displacement sensor based on diamond-shaped tapered split ring resonator," *IEEE Sens. J*., vol. 13, pp. 1153–1160, 2013.

[61] A. K. Horestani, D. Abbott, and C. Fumeaux, "Rotation sensor based on horn-shaped split ring resonator," *IEEE Sens. J.*, vol. 13, pp. 3014–3015, 2013.

[62] J. Naqui and F. Martín, "Transmission lines loaded with bisymmetric resonators and their application to angular displacement and velocity sensors," *IEEE Trans. Microw. Theory Techn*., vol. 61, no. 12, pp. 4700–4713, Dec. 2013.

[63] J. Naqui and F. Martín, "Angular displacement and velocity sensors based on electric-LC (ELC) loaded microstrip lines," *IEEE Sensors J.*, vol. 14, no. 4, pp. 939–940, Apr. 2014.

[64] A. K. Horestani, J. Naqui, D. Abbott, C. Fumeaux, and F. Martín, "Two-dimensional displacement and alignment sensor based on reflection coefficients of open microstrip lines loaded with split ring resonators," *Elec. Lett.*, vol. 50, pp. 620–622, Apr. 2014.

[65] A. Ebrahimi, W. Withayachumnankul, S. F. Al-Sarawi, and D. Abbott, "Metamaterial-inspired rotation sensor with wide dynamic range," *IEEE Sensors J*., vol. 14, no. 8, pp. 2609-2614, Aug. 2014.

[66] J. Naqui, J. Coromina, A. Karami-Horestani, C. Fumeaux, and F. Martín, "Angular displacement and velocity sensors based on coplanar waveguides (CPWs) loaded with S-shaped split ring resonator (S-SRR)," *Sensors*, vol. 15, pp. 9628–9650, 2015.

[67] J. Mata-Contreras, C. Herrojo, and F. Martín, "Application of split ring resonator (SRR) loaded transmission lines to the design of angular displacement and velocity sensors for space applications," *IEEE Trans. Microw. Theory Techn*., vol. 65, no. 11, pp. 4450-4460, Nov. 2017.

[68] J. Mata-Contreras, C. Herrojo, and F. Martín, "Detecting the rotation direction in contactless angular velocity sensors implemented with rotors loaded with multiple chains of split ring resonators (SRRs)," *IEEE Sensors J*., vol.18, no. 17, pp. 7055-7065, Sep. 2018.

[69] F. J. Ferrández-Pastor, J. M. García-Chamizo, and M. Nieto-Hidalgo, "Electromagnetic differential measuring method: application in microstrip sensors developing," *Sensors*, vol. 17, p. 1650, 2017.

[70] J. Muñoz-Enano, P. Vélez, M. Gil, and F. Martín, "An analytical method to implement high sensitivity transmission line differential sensors for dielectric constant measurements," *IEEE Sensors J.*, vol. 20, pp. 178-184, Jan. 2020.

[71] A. K. Jha, A. Lamecki, M. Mrozowski, and M. Bozzi, "A highly sensitive planar microwave sensor for detecting direction and angle of rotation," *IEEE Trans. Microw. Theory Techn*., vol. 68, no. 4, pp. 1598-1609, Apr. 2020.

[72] A. K. Horestani, Z. Shaterian, and F. Martín, "Rotation sensor based on the cross-polarized excitation of split ring resonators (SRRs)," *IEEE Sensors J*., published online. doi: 10.1109/JSEN.2020.2990484.

[73] J. Muñoz-Enano, P. Vélez, L. Su, M. Gil, P. Casacuberta, and F. Martín, "On the sensitivity of reflective-mode phase-variation sensors based on open-ended stepped-impedance transmission lines: theoretical analysis and experimental validation," *IEEE Trans. Microw. Theory Techn*., vol. 69, no. 1, pp. 308-324, Jan. 2021.

[74] L. Su, J. Muñoz-Enano, P. Vélez, P. Casacuberta, M. Gil, and F. Martín "Highly sensitive phase variation sensors based on step-impedance coplanar waveguide (CPW) transmission lines" *IEEE Sensors J*., vol. 21, no. 3, pp. 2864-2872, Feb. 2021.

[75] J. Muñoz-Enano, P. Vélez, L. Su, M. Gil, and F. Martín, "A reflective-mode phase-variation displacement sensor," *IEEE Access*, vol. 8, pp. 189565-189575, Oct. 2020.

[76] P. Casacuberta, J. Muñoz-Enano, P. Vélez, L. Su, M. Gil, and F. Martín, "Highly sensitive reflective-mode detectors and dielectric constant sensors based on open-ended stepped-impedance transmission lines," *Sensors*, vol. 20, paper 6236, 2020.

[77] J. Coromina, J. Muñoz-Enano, P. Vélez, A. Ebrahimi, J. Scott, K. Ghorbani, and F. Martín, "Capacitively-loaded slow-wave transmission lines for sensitivity improvement in phase-variation permittivity sensors," in *50th European Microwave Conference*, Utrecht, The Netherlands, Sep. 2020 (held virtually in Jan. 2021).

[78] A. Ebrahimi, J. Coromina, J. Muñoz-Enano, P. Vélez, J. Scott, K. Ghorbani, and F. Martín, "Highly sensitive phase-variation dielectric constant sensor based on a capacitively-loaded slow-wave transmission line," *IEEE Trans. Circ. Systems I*., submitted.

[79] J. Naqui, *Symmetry Properties in Transmission Lines Loaded with Electrically Small Resonators: Circuit Modeling and Applications*; Springer, Heidelberg, Germany, 2016.

[80] F. Martin, *Artificial Transmission Lines for RF and Microwave Applications*, John Wiley, Hoboken, NJ, USA, 2015.

[81] D.M. Pozar, *Microwave Engineering*, 4th Ed., John Wiley, Hoboken, NJ, USA, 2011.

[82] S. Mohammadi *et al*., "Gold coplanar waveguide resonator integrated with a microfluidic channel for aqueous dielectric detection," *IEEE Sensors J*., vol. 20, no. 17, pp. 9825-9833, Sep. 2020.

[83] M. Amirian, G. Karimi, B. D. Wiltshire, and M. H. Zarifi, "Differential narrow bandpass microstrip filter design for material and liquid purity interrogation," *IEEE Sensors J.*, vol. 19, no. 22, pp. 10545-10553, Nov. 2019.

[84] B. D. Wiltshire, S. Mohammadi, and M. H. Zarifi, "Integrating 3D printed microfluidic channels with planar resonator sensors for low cost and sensitive liquid detection," in *2018 18th International Symposium on Antenna Technology and Applied Electromagnetics (ANTEM)*, Waterloo, ON, 2018, pp. 1-2.

Lijuan Su was born in Qianjiang (Hubei), China in 1983. She received the B.S. degree in communication engineering and the M.S. degree in circuits and systems both from Wuhan University of Technology, Wuhan, China, in 2005 and 2013 respectively, and the Ph.D. degree in electronic engineering from Universitat Autonoma de Barcelona, Barcelona, Spain, in 2017. From Nov. 2017 to Dec. 2019, she worked as a postdoc researcher in Flexible Electronics Research Center, Huazhong University of Science and Technology, Wuhan, China. She is currently a postdoc researcher in CIMITEC, Universitat Autonoma de Barcelona, Spain. Her current research interests focus on the development of novel microwave sensors with improved performance for biosensors, dielectric characterization of solids and liquids, defect detection, industrial processes, etc.

Jonathan Muñoz-Enano was born in Mollet del Vallès (Barcelona), Spain, in 1994. He received the Bachelor's Degree in Electronic Telecommunications Engineering in 2016 and the Master's Degree in Telecommunications Engineering in 2018, both at the Autonomous University of Barcelona (UAB). Actually, he is working in the same university in the elaboration of his PhD, which is focused on the development of microwave sensors based on metamaterials concepts for the dielectric characterization of materials and biosensors.

Paris Vélez (S'10–M'14) was born in Barcelona, Spain, in 1982. He received the degree in Telecommunications Engineering, specializing in electronics, the Electronics Engineering degree, and the Ph.D. degree in Electrical Engineering from the Universitat Autònoma de Barcelona, Barcelona, in 2008, 2010, and 2014, respectively. His Ph.D. thesis concerned common mode suppression differential microwave circuits based on metamaterial concepts and semi-lumped resonators. During the Ph.D., he was awarded with a pre-doctoral teaching and research fellowship by the Spanish Government from 2011 to 2014. From 2015-2017, he was involved in the subjects related to metamaterials sensors for fluidics detection and characterization at LAAS-CNRS through a TECNIOSpring fellowship cofounded by the Marie Curie program. His current research interests include the miniaturization of passive circuits RF/microwave and sensors-based metamaterials through Juan de la Cierva fellowship. Dr. Vélez is a Reviewer for the IEEE Transactions on Microwave Theory and Techniques and for other journals.

Pau Casacuberta was born in Sabadell (Barcelona), Spain, in 1997. He received the Bachelor's Degree in Electronic Telecommunications Engineering and the Bachelor's Degree in Computer Engineering in 2020, both from the Universitat Autònoma de Barcelona (UAB). Currently, he is in his junior year of the Master's Degree in Telecommunications Engineering in the UAB. He received the Collaboration fellowship by the Spanish Government in 2019 for developing his Bachelor's Thesis in highly sensitive microwave sensors based in stepped impedance structures.

Marta Gil (S'05-M'09) was born in Valdepeñas, Ciudad Real, Spain, in 1981. She received the Physics degree from Universidad de Granada, Spain, in 2005, and the Ph.D. degree in electronic engineering from the Universitat Autònoma de Barcelona, Barcelona, Spain, in 2009. She studied one year with the Friedrich Schiller Universität Jena, Jena, Germany. During her PhD Thesis she was holder of a METAMORPHOSE NoE grant and National Research Fellowship from the FPU Program of the Education and Science Spanish Ministry. As a postdoctoral researcher, she was awarded with a Juan de la Cierva fellowship working in the Universidad de Castilla-La Mancha. She was postdoctoral researcher in the Institut für Mikrowellentechnik und Photonik in Technische Universität Darmstadt and in the Carlos III University of Madrid. She is currently associate professor in the Universidad Politécnica de Madrid. She has worked in metamaterials, piezoelectric MEMS and microwave passive devices. Her current interests include metamaterials sensors for fluidic detection.

Ferran Martín (M'04-SM'08-F'12) was born in Barakaldo (Vizcaya), Spain in 1965. He received the B.S. Degree in Physics from the Universitat Autònoma de Barcelona (UAB) in 1988 and the PhD degree in 1992. From 1994 up to 2006 he was Associate Professor in Electronics at the Departament d'Enginyeria Electrònica (Universitat Autònoma de Barcelona), and since 2007 he is Full Professor of Electronics. In recent years, he has been involved in different research activities including modelling and simulation of electron devices for high frequency applications, millimeter wave and THz generation systems, and the application of electromagnetic bandgaps to microwave and millimeter wave circuits. He is now very active in the field of metamaterials and their application to the miniaturization and optimization of microwave circuits and antennas. Other topics of interest include microwave sensors and RFID systems, with special emphasis on the development of high data capacity chipless-RFID tags. He is the head of the Microwave Engineering, Metamaterials and Antennas Group (GEMMA Group) at UAB, and director of CIMITEC, a research Center on Metamaterials supported by TECNIO (Generalitat de Catalunya). He has organized several international events related to metamaterials and related topics, including Workshops at the IEEE International Microwave Symposium (years 2005 and 2007) and European Microwave Conference (2009, 2015 and 2017), and the Fifth International Congress on Advanced Electromagnetic Materials in Microwaves and Optics (Metamaterials 2011), where he acted as Chair of the Local Organizing Committee. He has acted as Guest Editor for six Special Issues on metamaterials and sensors in five International Journals. He has authored and co-authored over 650 technical conference, letter, journal papers and book chapters, he is co-author of the book on Metamaterials entitled Metamaterials with Negative Parameters: Theory, Design and Microwave Applications (John Wiley & Sons Inc.), author of the book Artificial Transmission Lines for RF and Microwave Applications (John Wiley & Sons Inc.), co-editor of the book Balanced Microwave Filters (Wiley/IEEE Press) and co-author of the book Time-Domain Signature Barcodes for Chipless-RFID and Sensing Applications (Springer). Ferran Martín has generated 21 PhDs, has filed several patents on metamaterials and has headed several Development Contracts.

Prof. Martín is a member of the IEEE Microwave Theory and Techniques Society (IEEE MTT-S). He is reviewer of the IEEE Transactions on Microwave Theory and Techniques and IEEE Microwave and Wireless Components Letters, among many other journals, and he serves as member of the Editorial Board of IET Microwaves, Antennas and Propagation, International Journal of RF and Microwave Computer-Aided Engineering, and Sensors. He is also a member of the Technical Committees of the European Microwave Conference (EuMC) and International Congress on Advanced Electromagnetic Materials in Microwaves and Optics (Metamaterials). Among his distinctions, Ferran Martín has received the 2006 Duran Farell Prize for Technological Research, he holds the Parc de Recerca UAB – Santander Technology Transfer Chair, and he has been the recipient of three ICREA ACADEMIA Awards (calls 2008, 2013 and 2018). He is Fellow of the IEEE and Fellow of the IET.